*Journal of* ELECTRICAL ENGINEERING, VOL. 59, NO. 6, 2008, 294–301

# UNDERSTANDING DISCHARGE ACTIVITY DUE TO WATER DROPLET IN EPOXY NANOCOMPOSITES USING ACOUSTIC EMISSION TECHNIQUE

**Ramanujam Sarathi** [*] — **Michael G. Danikas** [**]

In the present study an attempt has been made to understand the characteristics/formation of corona/arcing discharges from water droplet under high electric field, in epoxy nanocomposites, adopting Acoustic Emission (AE) technique. The exfoliated/intercalated properties of the nanocomposites were analyzed through transmission electron microscopy (TEM) studies. It is observed that: corona initiated discharges are of intermittent process; low wt% of nanoclay content in epoxy resin reduces the surface carbonization due to arcing/corona discharges; gamma irradiation of epoxy nanocomposites have a great impact on the performance of the material. Based on AE studies, it could be concluded that the frequency content of AE signal generated due to arcing lies up to 250 kHz.

K e y w o r d s: arcing, corona, epoxy resin, insulation, nanocomposites, UHF signal, water droplet

## 1 INTRODUCTION

Nanocomposites are emerging as a new class of insulating materials for demanding applications in all electrical equipment used in the outdoor/indoor power system network [1, 2]. Polymeric insulators are preferred because of their better dielectric properties, low surface energy which maintains a good hydrophobic surface, better pollution performance in outdoor service condition, low weight, easy handling, vandal resistance, and cost effectiveness [3]. Recently, epoxy resin with organically modified clay filler has been used in major applications [4–8]. The selection of clay as a reinforcing material in epoxy resin is extremely appealing because of the cost, high thermal inertness, and environmentally friendly characteristics. It is believed that consistent improvements in the properties of clay loaded polymeric systems can be achieved by minimizing clay aggregation, promoting the formation of chemical bonds between polymer and clay and achieving exfoliation of clay. It is well known that certain amount of gamma irradiation could change the degree of polymerization and the fundamental properties of the material. Hence it is essential to understand the impact of gamma irradiation on the surface condition of the epoxy nanocomposite, for which the data base is scanty.

One of the major causes for corona inception in outdoor insulation structure is due to the presence of water droplets, which can initiate corona discharges followed by arcing leading to surface carbonization. Thus the formation of any incipient discharges/corona/partial discharges in the insulation structure can cause local perturbation in the steady medium due to release of certain amount of energy in the form of burst/impulsive pulses (acoustic energy), that radiate in all directions from the discharging source. The released energy can be detected by mounting the transducer over the surface of the structure. This process is known as *Acoustic emission* [9]. The signals detected are called acoustic signals, which are used for diagnostic study. Yong Zhu *et al*, studied the electrohydrodynamic activity of water droplet in silicone rubber insulation [10]. They have demonstrated that a locally high electric field at the tip of the droplet can trigger corona discharges. S.W. Rowland *et al* studied discharges between water droplets on silicone rubber insulation surface under AC voltages and concluded that the discharge process depends upon the magnitude of line current, resistivity of the moisture and the hydrophobic level of the insulation surface [11]. Suda *et al* established a method of monitoring whether flashover occurs or not in a string insulator based on leakage current waveforms and their frequency characteristics [12]. Sarathi *et al* adopted wavelet technique to understand the surface condition of insulation material due to tracking [13].

Having known all this in the present work, a methodical experimental study was carried out to understand the corona/arcing discharge that occurs from a water droplet over the surface of the epoxy nanocomposites. A wide band acoustic emission sensor placed over the surface of the insulating material and the AE signal generated due to corona/arcing were analysed. The influences of nanocomposites on AE signal generated were analysed. Also the impact of exfoliated/intercalated characteristics of epoxy nanocomposite material on surface discharges/corona was analyzed. The hydrophobicity of the material was characterized through contact angle measurements. The exfoliated/intercalated properties were analyzed through TEM studies.

[*] Department of Electrical Engineering, Indian Institute of Technology Madras, Chennai 600 036, India; rsarathi@iitm.ac.in
[**] Democritus University of Thrace, Department of Electrical and Computer Engineering., Electric Energy Systems Laboratory, 67 100 Xanthi, Greece; mdanikas@ee.duth.gr

ISSN 1335-3632 

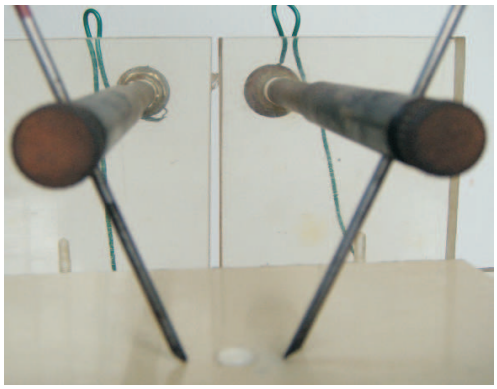

**Fig. 1.** Test Electrode Arrangement.

**Table 1.** Properties of Clay Particle.

| | |
|---|---|
| Colour | Off White |
| Bulk Density g/cc | 1.5–1.7 |
| Weight loss at 1000 °C | 37% |
| D spacing at $d_{001}$ | 17.2 |

## 2 EXPERIMENTAL STUDIES

Manufacturing epoxy nanocomposites is a major challenge and in the present work the nanocomposites were synthesized by high speed mechanical shear mixing of organo clay in the resin bath at room temperature. The clay mineral used in this study was organophillic MMT clay, procured from southern clay products Inc. (Gonzales, Texas) under the trade name of Garamite 1958. Table-I shows the physical properties of Garamite 1958 [14]. After uniform mixing of clay particles in epoxy resin (DGEBA, CY205, Ciba Geigy Inc), Tri Ethylene Tetra Amine (TETA) hardener was added and then cast in a mold of required dimension. Epoxy nanocomposites with different percentage of clay in the range 1–10 wt%, were prepared. Ultra thin films with thickness of about 80 nm for TEM observation was prepared by cutting the specimen using a glass knife with Leica ultracut UCT microtome. The sections were collected on carbon coated copper grids and kept in a desiccator before TEM studies (CM-12 Scanning transmission electron microscopy) to examine the morphology. The epoxy nanocomposite materials were exposed to gamma irradiation with a dose rate of 450 kRads/h. In the present study the specimens were exposed to 2000 kRads and 5000 kRads.

The test electrode setup used for investigating the behaviour of water droplets in an quasi-uniform electric field is shown in Fig. 1 The quasi-uniform electric field gap consists of two angular electrode tip cut for 45° (with smooth edges) placed on 3 mm thick epoxy nanocomposite material. The electrodes are separated by a gap distance of 15 mm. One electrode is connected to the AC high voltage source and the other electrode connected through a resistance of 1 kΩ to ground. The applied AC voltage measured using high AC voltage probe (LeCroy, USA model No.PPE20kV). The potential drop across the resistance fed directly to the digital storage oscilloscope to measure the discharge current characteristics. A 20 $\mu$l distilled water and 0.1N $NH_4Cl$ droplet of conductivity 2500 $\mu$S/cm were used for the discharge study. The AC voltage applied at the rate of 300 V/s till the discharge initiates between the droplet and the electrodes. The $NH_4Cl$ is used as standard solution (as suggested in IEC-60 587) while carrying out tracking test to understand the surface condition of insulation due to discharges [15]. The acoustic emission sensor is of wide band type manufactured by Physical Acoustics Ltd, USA. The droplet movements were photographed with Sony digital camera by operating it in movie mode (model No. DSC T100).

### 2.1 Acoustic Emission Instrumentation

The acoustic emission signal is basically a non-stationary signal. The amplitude and frequency content of the generated signal due to any defect vary depending on its location, intensity and medium in which it is propagating. The main problem in the acoustic emission signal analysis is the estimation of acoustic emission parameters. The sensors are piezoelectric transducers, which convert the acoustic signal into corresponding electric signals. The choice of the acoustic emission sensor depends on certain fundamental considerations. Electrical discharges generate acoustic activity across a very broad range of frequencies, from audible to several MHz. Two important aspects should be considered while choosing the frequency response of the detection transducer. They are interference from extraneous sources and the attenuation level of the signal in the medium in which it is propagating. The discharge characteristics which occurs at the surface of the insulating material is analyzed. In the present work, wide band sensor with the frequency response in the range 100 KHz–1 MHz was used in the study. To get maximum sensitivity, the sensor must be attached to the test specimen in such a manner that the acoustic energy passes into the transducer with minimum loss at the transducer material. The required contact achieved by applying thin layer of gel between the sensor and the surface of the chamber. On microscopic level the surface of the chamber will be rough and only few points will be in contact between the chamber and the sensor. The viscous gel will fill the gap and transfers the partial discharge produced acoustic energy to the surface of the sensor effectively. The silicon grease was used as the couplant. The sensor was placed at about 5 cm away from the discharge source by fixing it using rubber band.

The signal generated by the sensor has to be pre-amplified to the required voltage magnitude. Pre-amplifiers inevitably generate electronic noise, and it is the noise that sets the sensitivity of the acoustic emission system. The gain of the integrated pre-amplifier is set to 40 dB with a 1 MHz bandwidth. All the measurements were carried out with a threshold level of 40 db. The

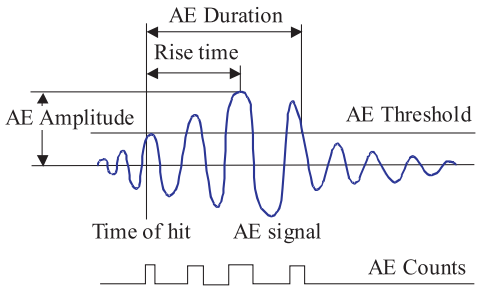


**Fig. 2.** Typical acoustic emission signal characteristics.

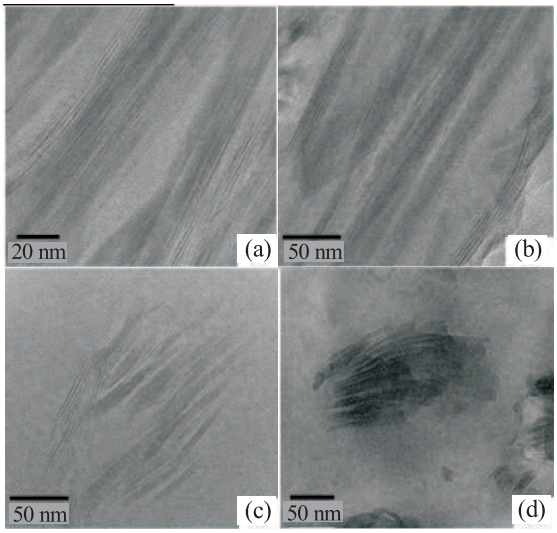


**Fig. 3.** TEM Patterns of Epoxy Nanocomposites (a) 1 % clay (b) 3 % clay (c) 5 % clay (d) 10 % clay.

PCI-2, 2 channel acoustic emission System of Physical Acoustic Corporation, USA is used.

Below some definitions of Acoustic Emission Signal Parameters are given [16]. It is essential to understand the phenomena based on the acoustic emission signal acquired through the AE sensor output. In the present work the arcing occurs between the water droplet and the electrodes. The PCI-2 AE system operates based on the hit principle. Figure 2 shows the typical acoustic emission hit features diagram. In the present work the amplitude, energy, counts and the rise time of the AE signals were measured to identify arcing characteristics.

*Amplitude* is the highest peak voltage reached by an AE waveform. This is an important parameter because it senses and identifies the AE events. The amplitude of the acoustic emissions are customarily expressed on a decibel scale, in which 1 $\mu$V at transducer is defined as 0 dB acoustic emission, 10 $\mu$V is 20 dB acoustic emission and so on. The amplitude of the AE signal depends on the magnitude of partial discharges occurring at the discharge site in the oil medium. *Rise time of the pulse* is defined as the time for the acoustic signal to reach maximum peak amplitude from the time instant it crosses the threshold, at every hit. *Duration of the pulse* is defined as the time from the point of crossing the threshold level till it cross back lower than the threshold setting. *Energy* of the signal is the measured area under the rectified signal envelope over the time. The energy measurement is preferred because it depends on the amplitude and the duration of the acoustic emission signal and is independent of threshold setting and operating frequency. The energy content of the signal is time varying and depends on the intensity of partial discharge formed. *Counts* are defined as the number of times the AE signal crosses the threshold in one inspection cycle. A 16 bit counter has been used in the system. It is capable of counting events in a single inspection cycle.

## 3 RESULTS AND DISCUSSION

### 3.1 Analysis of Morphology of Epoxy Nanocomposite Material

The dispersion of filler content in epoxy nanocomposites decides about its fundamental electrical, thermal and mechanical properties. Tanaka et al. carried out extensive study on nanocomposite material and concluded that the exfoliated structures have high performance [1]. Figure 3 shows the TEM images (showing intercalated/exfoliated structure) of the epoxy nanocomposites. The thick dark lines are the cross-section of the clay layers and grey white portions are the epoxy resin material. In an exfoliated structure, the layers of the clay have been completely separated and oriented in random in the base matrix [5]. It is observed that the prepared specimens are intercalated with partial exfoliation (Figs. 3a, b, c). From Fig. 3d it is realized that, as the weight percentage of clay is increased to 10 %, agglomeration occurs. In electrical insulation applications, the agglomerated zone acts as a charge trap site and interfacial discharges occurs leading to carbonization of material. Hence it is essential to have exfoliated nanocomposite structures.

### 3.2 Analysis of Hydrophobicity Level of Nanocomposites Using Contact Angle Measurements

The fundamental requirement of an insulating material used for outdoor/indoor applications is that it should have good water repellant characteristics. This could be easily characterized through contact angle measurement, which indicates level of hydrophobicity. If the contact angle of the material is above 90°, it is the indication that the material is hydrophobic and if the value is less than 90° it is the indication that the material is hydrophilic. The static contact angle was measured by liquid droplet method using distilled water [17]. The size of the drop was about 1.5 mm in diameter. The contact angle was measured using the following equation,

$$\theta = 2\tan^{-1}\frac{2h}{d} \tag{1}$$

where $d$ is the diameter of the liquid drop and $h$ is the height of the liquid drop. After the solution is placed

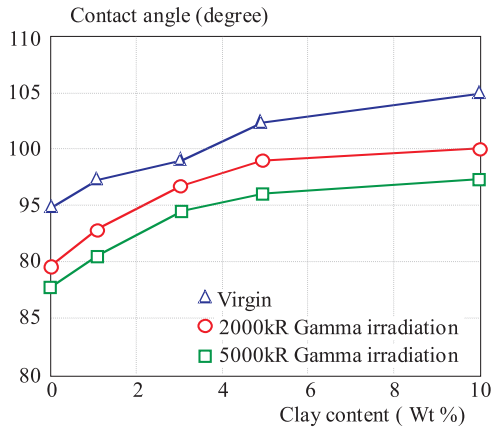


**Fig. 4.** Variation in contact angle of epoxy nanocomposites.

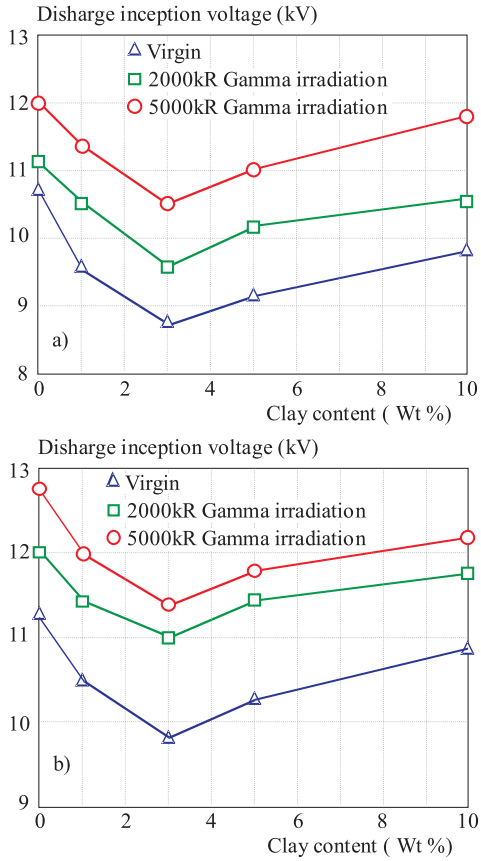


**Fig. 5.** Variation in Discharge inception voltage with epoxy nanocomposite aged with different dosage of gamma irradiation (a) distilled water (b) 0.1N ammonium chloride solution.

over the surface of the specimen, the height and diameter of the liquid droplet were measured within 5 seconds. Figure 4 shows variation in contact angle of the epoxy nanocomposites and for gamma irradiated specimens. For each specimen, the contact angle was measured at six different locations and averaged. It is realized that contact angle increases with increase in percentage of clay in epoxy nanocomposites, in the range studied. It is well known that increase in contact angle of the specimen reduces the wettability of the surface. It is observed that for a gamma irradiated specimen, increase in dosage shows reduction in contact angle of the specimen.

### 3.3 Understanding the discharge mechanism due to water droplet

When a droplet of water is placed in a strong electric field, it deforms to form a conical shape. The deformed water droplet will disrupt by the interaction of electrostatic force with the surface tension of the droplet, thereby a fraction of the droplet are ejected out from the tip of the cone initiating corona discharges. In the present work, the discharge inception voltage measured as voltage at once the transient discharge current is observed.

When an AC field is applied to liquid droplet, the shape of the droplet deforms with time depending on the frequency of the applied voltage. However, the droplet deforms strongly only at a particular frequency [11]. Electric field intensification along the triple point junctions of the insulation/air/water droplet contributes towards the liquid droplet deformation along the insulator surface and initiates discharges. The droplet of water placed on the surface of the insulating material and energized, it experiences tangential force, therefore the water droplet gets elongated along the surface. Figure 5 shows typical variation in discharge inception voltage when droplet of water of different conductivity, placed in the electrode gap over nanocomposite material, under AC voltages. It is realized that increase in percentage of clay in nanocomposite shows reduction in discharge inception voltage up to 3 wt% of clay and above which slight increase in discharge inception voltage is observed. Comparing the discharge inception voltage with distilled water and the ammonium chloride solution, it is realized that discharge inception voltage is high with water droplet of high conductivity. Figure 8 shows typical current signal measured during the discharge process. It could be realized that based on the magnitude of current signal, the evaporation time of the liquid varies. In the present study 20 MΩ is used as current limiting resistor.

To understand the surface condition of the insulating material, after the discharges, the droplets were allowed to evaporate by applying voltage of 16 kV. Figure 6 shows the variation in evaporation time of liquid droplet stressed under AC voltage with epoxy nanocomposites aged with different dosage of gamma irradiation

It is realized that the time for evaporation is high with epoxy nanocomposites up to 3 wt% of clay above which considerable reduction in evaporation is observed. Also by comparing the evaporation time of the droplet with distilled water and the ammonium chloride solution, it is realized that evaporation time is less with ammonium chloride solution.

In general, when the droplet is placed in a high electric field zone, corona discharge occurs and the surface tension becomes lower with the increase in temperature (due to corona discharges) at the edge of water droplet, tending to zero at the discharge root. The water will protrude from the drop at the discharge root causing continuous discharges between the water droplets and the edges of

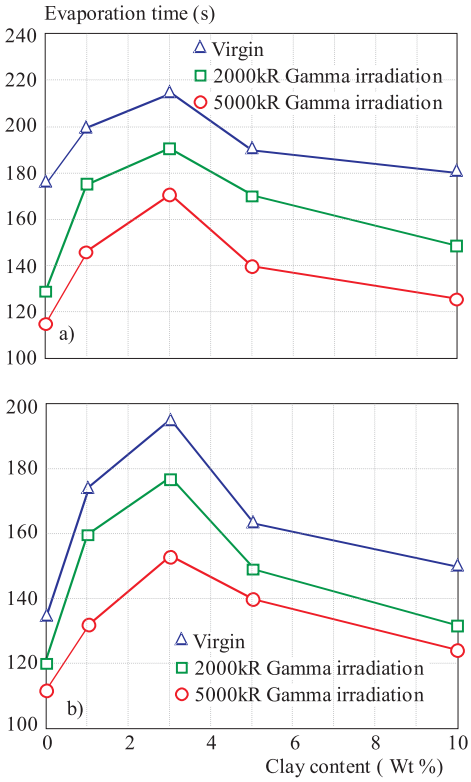


**Fig. 6.** Variation in evaporation time of liquid droplet stressed under AC voltage with epoxy nanocomposites aged with different dosage of gamma irradiation (a) distilled water (b) 0.1N ammonium chloride solution


**Fig. 7.** Typical photograph showing arcing between electrodes and water droplets in a 10 Wt% of clay in epoxy nanocomposites

two electrodes as shown in Fig. 7. The voltage and current measured at the instant of corona formation and during continuous arcing/discharges is shown in Figs. 8a and 8b, respectively. When the two electrodes are bridged by water droplet forming thin film only the resistive current flows as could be realized from Fig. 8c.

### 3.4 Influence of gamma Irradiation on Surface Condition of Insulating Material

It is realized from Fig. 5 and Fig. 6 that the increase in dosage of gamma irradiation shows an increase in discharge inception voltage and reduction in evaporation time. The condition is the same with the distilled water and ammonium chloride solution. It could be realized by comparing the static contact angle of the insulation surface with the discharge inception voltage, it shows inverse relationship up to 3 wt%.

### 3.5 Analysis of AE Signals Measured During Arcing

Figure 9 shows a typical AE signal generated due to arc discharges between water droplet and electrodes under AC voltages. It is observed that impulsive type signal gets generated due to arcing. Also it is noticed that the characteristics of signal have not changed due to different percentage of clay in epoxy nanocomposites. Figure 9b shows the corresponding FFT of the AE signal. It could be realized that the frequency content of the AE signal generated due to arcing have frequency content up to 250 kHz.

Figure 10 shows variation in magnitude of AE signal measured at different instants of time from the point of inception of corona from liquid droplet and at the time of evaporation of liquid droplets. It is observed that AE signal could be recognized once corona signal emanates from the liquid droplet (which is the first stage) followed with arcing between the two electrodes touching the upper meniscus of the water droplet. During this period it is observed that the magnitude of AE signal is high. In this process the temperature rise at the surface of the material between water droplet and the electrodes occurs, causing degradation of surface, thereby reducing the contact angle, allowing the water to flow near to the electrodes, thereby enhancing the local electric field causing sustained discharges between the edges of the water and the electrodes causing evaporation of liquid droplet (Stage (iii)) During this process, the acoustic signal magnitudes are much lower than the arcing between the electrodes. Once the water droplet evaporates, at the time of termination of discharges direct arc discharge between two electrodes occurs causing increased AE signal magnitude. Thus measurement of AE signal helps one to correlate the process of discharge that occurs due to water droplet under high electric fields.

In the present work, the mechanism of inception of discharge and evaporation of liquid is almost the same, irrespective of percentage of clay in epoxy nanocomposites. The AE signals generated due to arcing in materials with higher percentage of clay in epoxy nanocomposite material show a reduction in their magnitudes. This could be due to damping effect of clay particle in the base material, which absorbs certain amount of energy content. Also it could be observed that, for gamma irradiated specimen, the AE signal magnitude is high irrespective of percentage of clay in epoxy nanocomposites compared to virgin

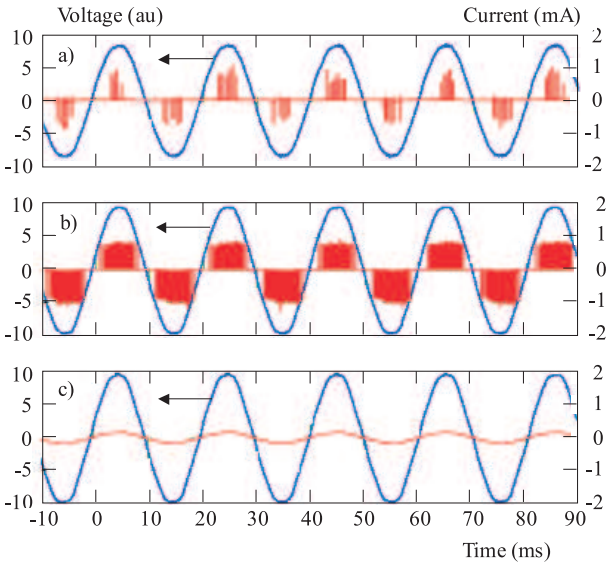


**Fig. 8.** Typical voltage and current measured at different instant of time (a) corona inception (b) during arc discharge (c) resistive current flow due to bridging of electrodes

specimen. The cause for it has to be understood by carrying out certain physico- chemical diagnostic studies.

The other parameters viz. rise time, duration, energy content and counts of AE signal formed due to different stages of discharges formed due to water droplet are shown in Figs. 11 to 14, respectively. It is realized that count, energy and duration of the signal increases with increase in percentage of clay up to 3 wt% of clay above which a drastic reduction in their values were observed. In the case of risetime of AE signal generated, it could be realized that increase in percentage of clay content up to 3 wt% shows less rise time and above which characteristic increase in rise time is observed. Thus it could be realized that the quantity of filler content present in the nano-composite material varies the characteristics of AE signal generated during corona formation/arcing period. Also it could be realized based on the present study (from Figs. 10 to 14) that the characteristics of AE signal generated in a gamma irradiated specimen, especially the counts, duration and energy contents are high compared to the virgin specimen. In addition, the higher surface damage increases the parametric values of the AE signal generated. Thus the AE technique proves to be a diagnostic tool for condition monitoring the surface condition of the insulating material during operation. The AE technique proved also to be a very useful tool for the characterization of partial discharges in transformer oil insulation under both AC and DC voltages [18]. It seems that the AE technique is of significant value as a diagnostic tool for both liquid and solid insulants.

## 4 CONCLUSIONS

The important conclusions arrived at, based on the present study, are the following:

1. TEM analysis of epoxy nanocomposite material indicates that up to 5 wt% of clay content in epoxy resin forms partially exfoliated structure. The contact angle of the insulating material increases with increase in percentage of clay in epoxy nanocomposite.

2. Increase in percentage of clay content in epoxy resin shows reduction in discharge inception time up to 3 wt%. The evaporation of volume of liquid shows increase in time with increase in percentage of clay content of up to 3 wt%.

3. It is observed that evaporation rate of ammonium chloride solution droplet is high compared with the distilled water. This indicates that conductivity of the droplet has a major role on discharge inception and on the level of damage of the insulation material.

4. It is observed that gamma irradiated specimen shows reduction in contact angle compared to virgin specimen. It is also observed that increase in gamma irradiation dosage shows characteristic reduction in the contact angle. The discharge inception voltage of the gamma irradiated specimen is high compared to virgin specimen. The evaporation time of the liquid droplet placed over gamma irradiated specimen shows a reduction in its value compared to virgin specimen.

5. The amplitudes of AE signal generated by the discharges from water on the surface of epoxy nanocomposites under high fields are time varying. In general arcing

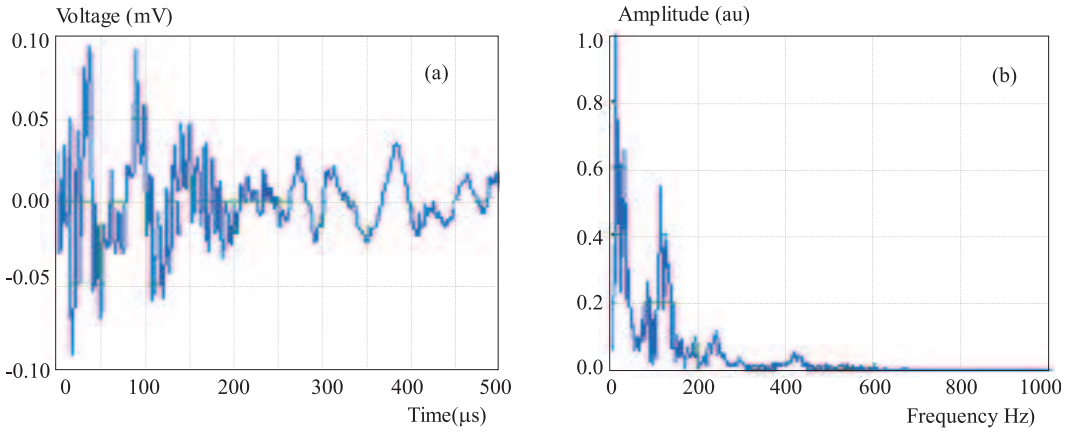


**Fig. 9.** Typical (a) acoustic emission signal generated during arcing (b) normalized FFT of (a)

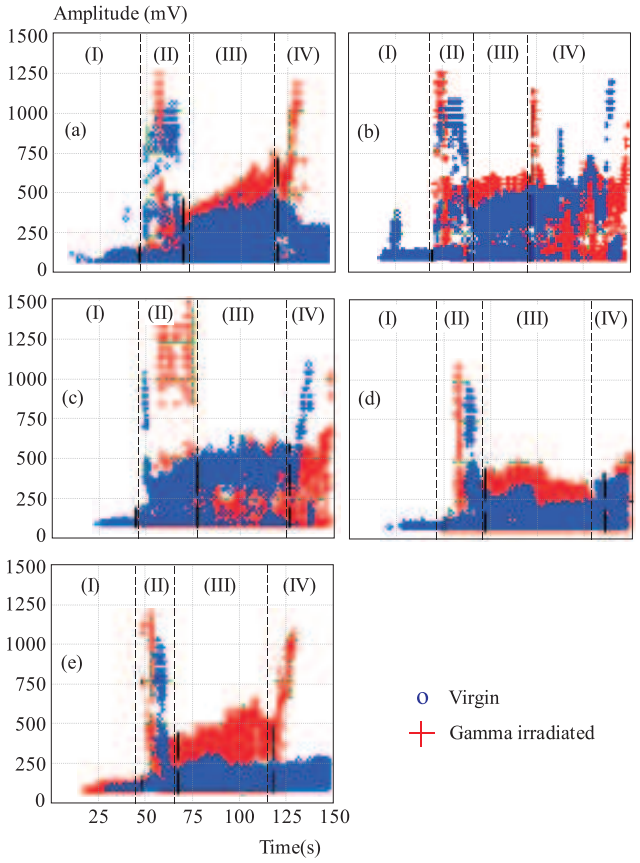


**Fig. 10.** Variation in Amplitude of AE signal generated due to corona/arcing in nanocomposite material under AC voltages (a) 0% (b) 1% (c) 3% (d) 5% (e) 10%.

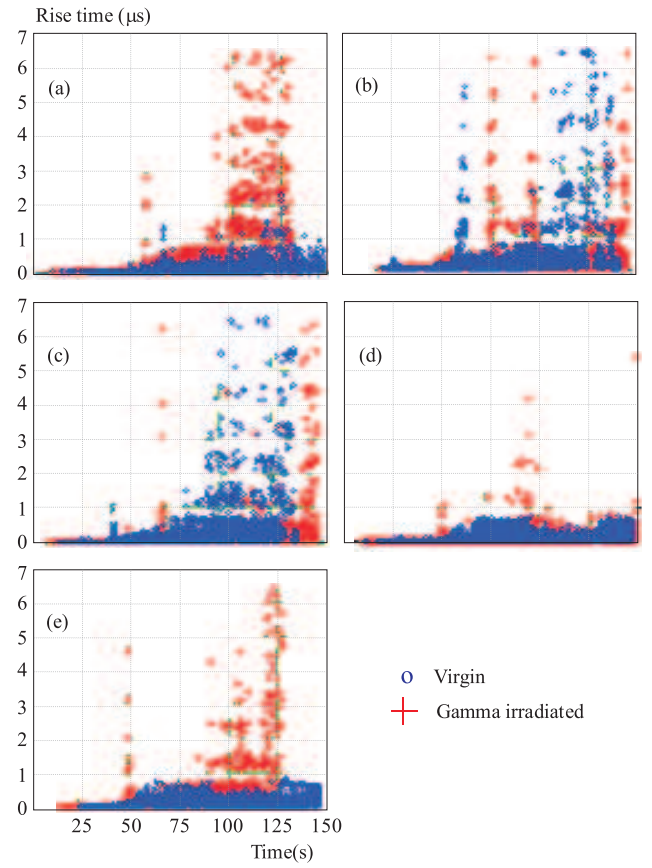


**Fig. 11.** Variation in rise time of AE signal generated due to corona/arcing in nanocomposite material under AC voltages (a) 0% (b) 1% (c) 3% (d) 5% (e) 10%.

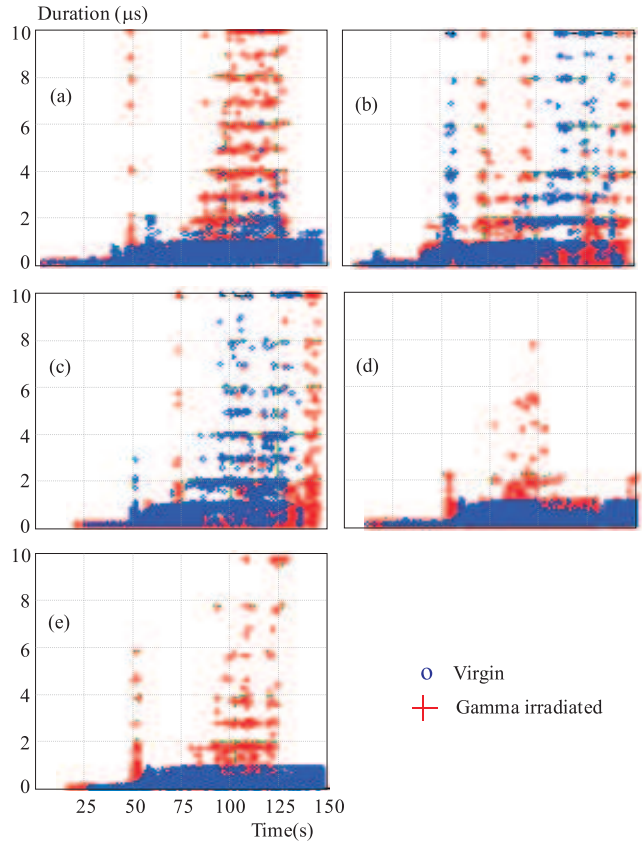


**Fig. 12.** Variation in duration of AE signal generated due to corona/arcing in nanocomposite material under AC voltages (a) 0% (b) 1% (c) 3% (d) 5% (e) 10%

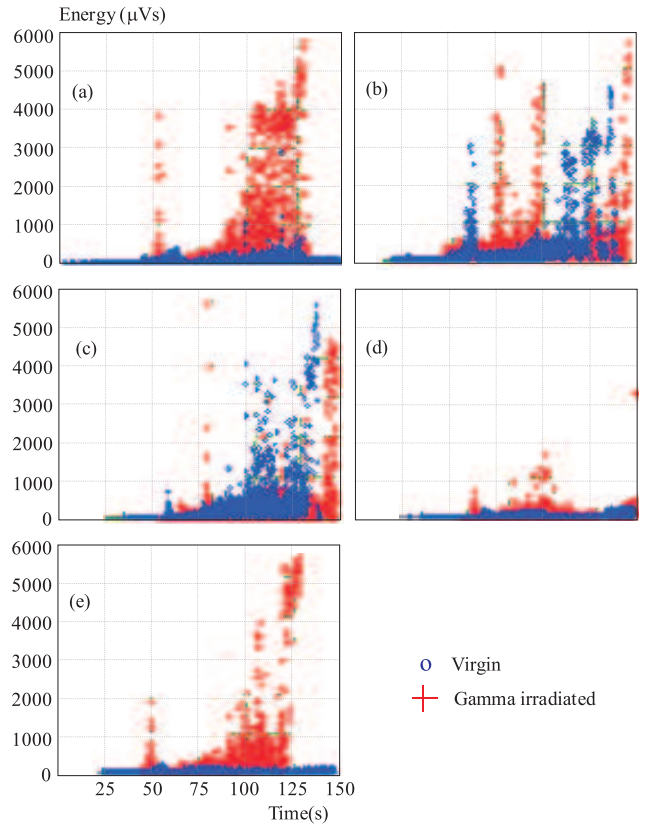


**Fig. 13.** Variation in rise time of AE signal generated due to corona/arcing in nanocomposite material under AC voltages (a) 0% (b) 1% (c) 3% (d) 5% (e) 10%

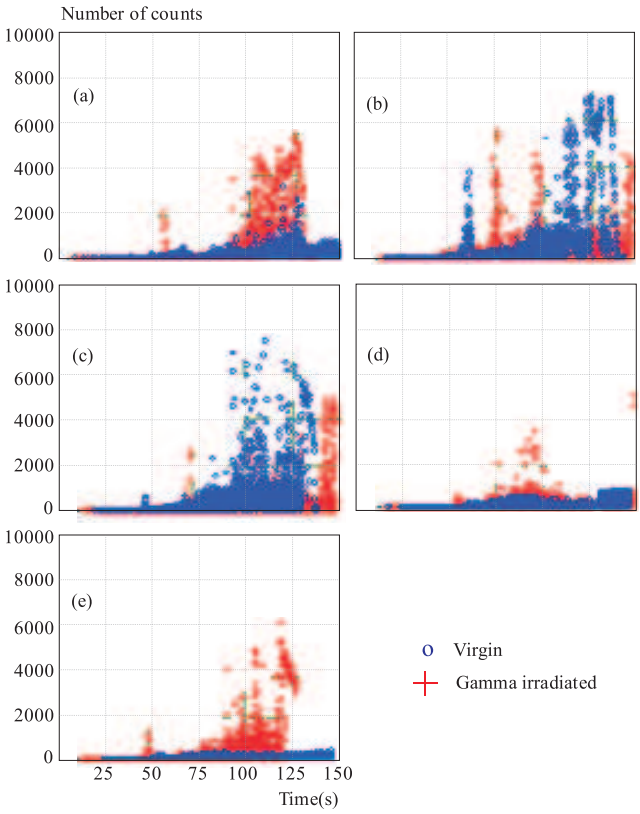


**Fig. 14.** Variation in number of counts of AE signal generated due to corona/arcing in nanocomposite material under AC voltages (a) 0% (b) 1% (c) 3% (d) 5% (e) 10%.

between two electrodes generates high magnitude of AE signal compared with the continuous arcing between the water droplet and the electrodes. Also the amplitude of AE signal generated due to arcing between water droplet and electrodes are high in the gamma irradiated specimens compared to the virgin specimen.

6. The parameters of the AE signal viz the count, duration and the energy content are high with the gamma irradiated specimen compared with the virgin specimen. Correlating the evaporation time and the parameters of the AE signal generated, a lower evaporation time of the liquid droplet shows an increase in parametric values of the AE signal, confirming AE technique as suitable diagnostic tool for condition monitoring the surface condition of the insulating material during operation, for any discharges.

7. It is realized that arcing initiated from liquid droplet on the surface of epoxy nanocomposite insulating material generates AE signal and the frequency content of it is less than 250 kHz, irrespective of percentage of clay in epoxy nanocomposite material and for gamma irradiated specimen.

**Acknowledgements**

The author wish to thank Ms Abirami and Mr G. Nagesh for helping the author (RS) for carrying out the Acoustic emission study.

## References

[1] TANAKA, T.—MONTANARI, G. C.—MULHAUPT, R.: Polymer Nanocomposites as Dielectrics and Electrical Insulation — Perspectives for Processing Technologies, Material Characterization and Future Applications, IEEE Trans. Dielectrics and Electrical Insulation **11** (2004), 763–784.

[2] KOZAKO, M.—FUSE, N.—OHKI, Y.—OKAMOTO, T.—TANAKA, T.: Surface Degradation of Polyamide Nanocomposites Caused by Partial Discharges Using IEC (b) Electrodes, IEEE Trans. Dielectrics and Electrical Insulation **11** (2004), 833–839.

[3] GORUR, R. S.—CHERNEY, E. A.—BURNHAM, J. T.: Outdoor Insulators, Ravi S. Gorur, Inc., Phoenix, Arizona 85044, USA, 1999.

[4] LAN, T.—PINNAVAIA, T. J.: Clay-Reinforced Epoxy Nanocomposites, Chemistry of Materials **6** (1994), 2216–2219.

[5] PINNAVAIA, T. J.—BEALL, G. W.: Polymer-Clay Nanocomposites, Wiley Series in Polymer Science, New York, 2000.

[6] ZILG, C.—MULHAUPT, R.—FINTER, J.: Morphology and Toughness/Stiffness Balance of nanocomposites based Upon Anhydride-Cured Epoxy Resins and Layered Silicates, Macromol. Chem. Phys. **200** (1999), 661–670.

[7] ALEXANDRE, M.—DUBOIS, P.: Polymer-Layered Silicate nanocomposites: Preparation, Properties and Uses of a New Class of Materials, Materials Science and Engineering **28** (2000), 1–63.

[8] MESSERSMITH, P. B.—GIANNELIS, E. P.: Synthesis and Characterization of layered Silicate-Epoxy Nanocomposites, Chemistry of Materials **6** (1994), 1719–1725.

[9] HUNTER, J. L.: Acoustics, Eds. Prentice Hall Inc., 1957.

[10] ZHU, Y.—HAJI, K.—OTSUBO, M.—HONDA, C.—HAYASHI, N.: Electrohydrodynamic Behavior of Water Droplet on an Electrically Stressed Hydrophobic Surface, J. Phys. D: Appl. Phys. **39** (2006), 1970–1975.

[11] ROWLAND, S. W.—LIN, F. C.: Stability of Alternating Current Discharges between Water Drops on Insulation Surfaces, J. Appl. D: Appl. Phys. **39** (2006), 3067–3076.

[12] SUDA, T.: Frequency Characteristics of Leakage Current Waveforms of an Artificially Polluted Suspension Insulator, IEEE Transactions on Dielectrics and Electrical Insulation **8** (2001), 705–709.

[13] SARATHI, R.—CHANDRASEKAR, S.—YOSHIMURA, N.: Investigation of Surface Condition of Outdoor Insulation Material using Wavelets, IEEE Trans. on Power Delivery **21** (2006), 515–516.

[14] Southern Clay Products., Inc, Technical data.

[15] IEC Publication 60 587. Testing Method for Evaluating the Resistance of Tracking and Erosion of Electrical Insulating Materials Used under Severe Ambient Conditions,1984.

[16] POLLOCK, A. A.: Acoustic Emission Inspection, Physical Acoustics Corporation, Technical Report TR-103-96-12/89.

[17] CRANK, J.: Mathematics of Diffusion, 2nd edition, Eds. Clarendon, Oxford, 1975.

[18] SARATHI, R.—SINGH, P. D.—DANIKAS, M. G.: Characterization of Partial Discharges in Transformer Oil Insulation Under AC and DC Voltage Using Acoustic Emission Technique, J. Electr. Eng. **58** (2007), 91–97.

Received 26 August 2008

**Ramanujam Sarathi** and **Michael G. Danikas**, biographies not supplied.